EUROPEAN LABORATORY FOR PARTICLE PHYSICS (CERN)

CERN-EP/99-086
June 28, 1999

A Study of Single W Production in e^+e^- Collisions at $\sqrt{s} = 161 - 183$ GeV

The ALEPH Collaboration*)

Abstract

Single W production is studied in the data recorded with the ALEPH detector at LEP at centre-of-mass energies between 161 and 183 GeV. The cross section is measured to be $\sigma_{\mathrm{W}} = 0.41 \pm 0.17(\mathrm{stat.}) \pm 0.04(\mathrm{syst.})$ pb at 183 GeV, consistent with the Standard Model expectation. Limits on non-standard WWγ couplings are deduced as $-1.6 < \kappa_\gamma < 1.5$ ($\lambda_\gamma = 0$) and $-1.6 < \lambda_\gamma < 1.6$ ($\kappa_\gamma = 1$) at 95% C.L. A search for effectively invisible decays of the W boson in W pair production is performed, leading to an upper limit on the branching ratio of 1.3% ($\Gamma_{\mathrm{inv}} = 27$ MeV) at 95% C.L.

(Submitted to Physics Letters B)

*) See next pages for the list of authors.

The ALEPH Collaboration

R. Barate, D. Decamp, P. Ghez, C. Goy, S. Jezequel, J.-P. Lees, F. Martin, E. Merle, M.-N. Minard, B. Pietrzyk, H. Przysiezniak

Laboratoire de Physique des Particules (LAPP), IN^{2}P^3-CNRS, F-74019 Annecy-le-Vieux Cedex, France

R. Alemany, M.P. Casado, M. Chmeissani, J.M. Crespo, E. Fernandez, M. Fernandez-Bosman, Ll. Garrido,[15] E. Graugès, A. Juste, M. Martinez, G. Merino, R. Miquel, Ll.M. Mir, P. Morawitz, A. Pacheco, I.C. Park, I. Riu

Institut de Física d'Altes Energies, Universitat Autònoma de Barcelona, 08193 Bellaterra (Barcelona), E-Spain[7]

A. Colaleo, D. Creanza, M. de Palma, G. Iaselli, G. Maggi, M. Maggi, S. Nuzzo, A. Ranieri, G. Raso, F. Ruggieri, G. Selvaggi, L. Silvestris, P. Tempesta, A. Tricomi,[3] G. Zito

Dipartimento di Fisica, INFN Sezione di Bari, I-70126 Bari, Italy

X. Huang, J. Lin, Q. Ouyang, T. Wang, Y. Xie, R. Xu, S. Xue, J. Zhang, L. Zhang, W. Zhao

Institute of High-Energy Physics, Academia Sinica, Beijing, The People's Republic of China[8]

D. Abbaneo, U. Becker,[19] G. Boix,[6] M. Cattaneo, F. Cerutti, V. Ciulli, G. Dissertori, H. Drevermann, R.W. Forty, M. Frank, F. Gianotti, T.C. Greening, A.W. Halley, J.B. Hansen, J. Harvey, P. Janot, B. Jost, I. Lehraus, O. Leroy, C. Loomis, P. Maley, P. Mato, A. Minten, A. Moutoussi, F. Ranjard, L. Rolandi, D. Schlatter, M. Schmitt,[20] O. Schneider,[2] P. Spagnolo, W. Tejessy, F. Teubert, I.R. Tomalin, E. Tournefier, A.E. Wright

European Laboratory for Particle Physics (CERN), CH-1211 Geneva 23, Switzerland

Z. Ajaltouni, F. Badaud G. Chazelle, O. Deschamps, S. Dessagne, A. Falvard, C. Ferdi, P. Gay, C. Guicheney, P. Henrard, J. Jousset, B. Michel, S. Monteil, J-C. Montret, D. Pallin, P. Perret, F. Podlyski

Laboratoire de Physique Corpusculaire, Université Blaise Pascal, IN^{2}P^3-CNRS, Clermont-Ferrand, F-63177 Aubière, France

J.D. Hansen, J.R. Hansen, P.H. Hansen, B.S. Nilsson, B. Rensch, A. Wäänänen

Niels Bohr Institute, 2100 Copenhagen, DK-Denmark[9]

G. Daskalakis, A. Kyriakis, C. Markou, E. Simopoulou, A. Vayaki

Nuclear Research Center Demokritos (NRCD), GR-15310 Attiki, Greece

A. Blondel, J.-C. Brient, F. Machefert, A. Rougé, M. Swynghedauw, R. Tanaka, A. Valassi,[23] H. Videau

Laboratoire de Physique Nucléaire et des Hautes Energies, Ecole Polytechnique, IN^{2}P^3-CNRS, F-91128 Palaiseau Cedex, France

E. Focardi, G. Parrini, K. Zachariadou

Dipartimento di Fisica, Università di Firenze, INFN Sezione di Firenze, I-50125 Firenze, Italy

R. Cavanaugh, M. Corden, C. Georgiopoulos

Supercomputer Computations Research Institute, Florida State University, Tallahassee, FL 32306-4052, USA [13,14]

A. Antonelli, G. Bencivenni, G. Bologna,[4] F. Bossi, P. Campana, G. Capon, V. Chiarella, P. Laurelli, G. Mannocchi,[1,5] F. Murtas, G.P. Murtas, L. Passalacqua, M. Pepe-Altarelli[1]

Laboratori Nazionali dell'INFN (LNF-INFN), I-00044 Frascati, Italy

M. Chalmers, L. Curtis, J.G. Lynch, P. Negus, V. O'Shea, B. Raeven, C. Raine, D. Smith, P. Teixeira-

Dias, A.S. Thompson, J.J. Ward

Department of Physics and Astronomy, University of Glasgow, Glasgow G12 8QQ,United Kingdom[10]

O. Buchmüller, S. Dhamotharan, C. Geweniger, P. Hanke, G. Hansper, V. Hepp, E.E. Kluge, A. Putzer, J. Sommer, K. Tittel, S. Werner,[19] M. Wunsch

Institut für Hochenergiephysik, Universität Heidelberg, D-69120 Heidelberg, Germany[16]

R. Beuselinck, D.M. Binnie, W. Cameron, P.J. Dornan,[1] M. Girone, S. Goodsir, N. Marinelli, E.B. Martin, J. Nash, J. Nowell, A. Sciabà, J.K. Sedgbeer, E. Thomson, M.D. Williams

Department of Physics, Imperial College, London SW7 2BZ, United Kingdom[10]

V.M. Ghete, P. Girtler, E. Kneringer, D. Kuhn, G. Rudolph

Institut für Experimentalphysik, Universität Innsbruck, A-6020 Innsbruck, Austria[18]

C.K. Bowdery, P.G. Buck, G. Ellis, A.J. Finch, F. Foster, G. Hughes, R.W.L. Jones, N.A. Robertson, M. Smizanska, M.I. Williams

Department of Physics, University of Lancaster, Lancaster LA1 4YB, United Kingdom[10]

I. Giehl, F. Hölldorfer, K. Jakobs, K. Kleinknecht, M. Kröcker, A.-S. Müller, H.-A. Nürnberger, G. Quast, B. Renk, E. Rohne, H.-G. Sander, S. Schmeling, H. Wachsmuth C. Zeitnitz, T. Ziegler

Institut für Physik, Universität Mainz, D-55099 Mainz, Germany[16]

J.J. Aubert, C. Benchouk, A. Bonissent, J. Carr,[1] P. Coyle, A. Ealet, D. Fouchez, F. Motsch, P. Payre, D. Rousseau, M. Talby, M. Thulasidas, A. Tilquin

Centre de Physique des Particules, Faculté des Sciences de Luminy, IN^2*P*^{3}*-CNRS, F-13288 Marseille, France*

M. Aleppo, M. Antonelli, F. Ragusa

Dipartimento di Fisica, Università di Milano e INFN Sezione di Milano, I-20133 Milano, Italy.

V. Büscher, H. Dietl, G. Ganis, K. Hüttmann, G. Lütjens, C. Mannert, W. Männer, H.-G. Moser, S. Schael, R. Settles, H. Seywerd, H. Stenzel, W. Wiedenmann, G. Wolf

Max-Planck-Institut für Physik, Werner-Heisenberg-Institut, D-80805 München, Germany[16]

P. Azzurri, J. Boucrot, O. Callot, S. Chen, M. Davier, L. Duflot, J.-F. Grivaz, Ph. Heusse, A. Jacholkowska,[1] M. Kado, J. Lefrançois, L. Serin, J.-J. Veillet, I. Videau,[1] J.-B. de Vivie de Régie, D. Zerwas

Laboratoire de l'Accélérateur Linéaire, Université de Paris-Sud, IN^2*P*^{3}*-CNRS, F-91898 Orsay Cedex, France*

G. Bagliesi, S. Bettarini, T. Boccali, C. Bozzi,[12] G. Calderini, R. Dell'Orso, I. Ferrante, A. Giassi, A. Gregorio, F. Ligabue, A. Lusiani, P.S. Marrocchesi, A. Messineo, F. Palla, G. Rizzo, G. Sanguinetti, G. Sguazzoni, R. Tenchini, C. Vannini, A. Venturi, P.G. Verdini

Dipartimento di Fisica dell'Università, INFN Sezione di Pisa, e Scuola Normale Superiore, I-56010 Pisa, Italy

G.A. Blair, J. Coles, G. Cowan, M.G. Green, D.E. Hutchcroft, L.T. Jones, T. Medcalf, J.A. Strong, J.H. von Wimmersperg-Toeller

Department of Physics, Royal Holloway & Bedford New College, University of London, Surrey TW20 OEX, United Kingdom[10]

D.R. Botterill, R.W. Clifft, T.R. Edgecock, P.R. Norton, J.C. Thompson

Particle Physics Dept., Rutherford Appleton Laboratory, Chilton, Didcot, Oxon OX11 OQX, United Kingdom[10]

B. Bloch-Devaux, P. Colas, B. Fabbro, G. Faïf, E. Lançon, M.-C. Lemaire, E. Locci, P. Perez, J. Rander, J.-F. Renardy, A. Rosowsky, A. Trabelsi,[21] B. Tuchming, B. Vallage
CEA, DAPNIA/Service de Physique des Particules, CE-Saclay, F-91191 Gif-sur-Yvette Cedex, France[17]

S.N. Black, J.H. Dann, H.Y. Kim, N. Konstantinidis, A.M. Litke, M.A. McNeil, G. Taylor
Institute for Particle Physics, University of California at Santa Cruz, Santa Cruz, CA 95064, USA[22]

C.N. Booth, S. Cartwright, F. Combley, P.N. Hodgson, M.S. Kelly, M. Lehto, L.F. Thompson
Department of Physics, University of Sheffield, Sheffield S3 7RH, United Kingdom[10]

K. Affholderbach, A. Böhrer, S. Brandt, C. Grupen, J. Hess, A. Misiejuk, G. Prange, U. Sieler
Fachbereich Physik, Universität Siegen, D-57068 Siegen, Germany[16]

G. Giannini, B. Gobbo
Dipartimento di Fisica, Università di Trieste e INFN Sezione di Trieste, I-34127 Trieste, Italy

J. Putz, J. Rothberg, S. Wasserbaech, R.W. Williams
Experimental Elementary Particle Physics, University of Washington, WA 98195 Seattle, U.S.A.

S.R. Armstrong, P. Elmer, D.P.S. Ferguson, Y. Gao, S. González, O.J. Hayes, H. Hu, S. Jin, P.A. McNamara III, J. Nielsen, W. Orejudos, Y.B. Pan, Y. Saadi, I.J. Scott, J. Walsh, Sau Lan Wu, X. Wu, G. Zobernig
Department of Physics, University of Wisconsin, Madison, WI 53706, USA[11]

---

[1]Also at CERN, 1211 Geneva 23, Switzerland.
[2]Now at Université de Lausanne, 1015 Lausanne, Switzerland.
[3]Also at Centro Siciliano di Fisica Nucleare e Struttura della Materia, INFN Sezione di Catania, 95129 Catania, Italy.
[4]Also Istituto di Fisica Generale, Università di Torino, 10125 Torino, Italy.
[5]Also Istituto di Cosmo-Geofisica del C.N.R., Torino, Italy.
[6]Supported by the Commission of the European Communities, contract ERBFMBICT982894.
[7]Supported by CICYT, Spain.
[8]Supported by the National Science Foundation of China.
[9]Supported by the Danish Natural Science Research Council.
[10]Supported by the UK Particle Physics and Astronomy Research Council.
[11]Supported by the US Department of Energy, grant DE-FG0295-ER40896.
[12]Now at INFN Sezione di Ferrara, 44100 Ferrara, Italy.
[13]Supported by the US Department of Energy, contract DE-FG05-92ER40742.
[14]Supported by the US Department of Energy, contract DE-FC05-85ER250000.
[15]Permanent address: Universitat de Barcelona, 08208 Barcelona, Spain.
[16]Supported by the Bundesministerium für Bildung, Wissenschaft, Forschung und Technologie, Germany.
[17]Supported by the Direction des Sciences de la Matière, C.E.A.
[18]Supported by Fonds zur Förderung der wissenschaftlichen Forschung, Austria.
[19]Now at SAP AG, 69185 Walldorf, Germany
[20]Now at Harvard University, Cambridge, MA 02138, U.S.A.
[21]Now at Département de Physique, Faculté des Sciences de Tunis, 1060 Le Belvédère, Tunisia.
[22]Supported by the US Department of Energy, grant DE-FG03-92ER40689.
[23]Now at LAL, 91898 Orsay, France.

1 Introduction

The Standard Model has been tested to high accuracy at LEP, CERN's large e^+e^- collider operating at centre-of-mass energies near the Z boson resonance [1]. The increase of LEP's centre-of-mass energy beyond the W pair production threshold offers an opportunity to study the properties of the W boson and search for new physics.

The measurement of the trilinear gauge boson couplings (TGC) is an important test of their non-Abelian nature. In this paper the notation of [2] is followed, where the C and P conserving couplings are denoted as $\Delta g_1^{\mathrm{Z}} = g_1^{\mathrm{Z}} - 1$, κ_γ, κ_{Z}, λ_γ and λ_{Z}, where γ (Z) refers to the WWγ (ZWW) vertex. In the Standard Model $\kappa_\gamma = \kappa_{\mathrm{Z}} = 1$ while all other couplings are zero. The couplings describing the WWγ vertex can be related to the magnetic dipole moment $\mu_{\mathrm{W}} = e/(2m_{\mathrm{W}})(1 + \kappa_\gamma + \lambda_\gamma)$, and the electric quadrupole moment: $Q_{\mathrm{W}} = -e/m_{\mathrm{W}}^2(\kappa_\gamma - \lambda_\gamma)$ [3]. While the couplings have been measured in W pair production [4, 5, 6, 7], the WWZ vertex cannot be distinguished from the WWγ vertex in these measurements.

Single W production offers a clean access to the couplings of the WWγ vertex, in particular to κ_γ [8]. The measurement of the production cross section, presented in this paper, is sensitive to the couplings and thus limits can be set on new physics parametrised by the WWγ couplings.

Supersymmetric extensions of the Standard Model predict in particular charginos, the supersymmetric partners of the charged gauge and Higgs bosons, neutralinos, the partners of the neutral gauge and Higgs bosons, and sneutrinos, partners of the neutrinos [9]. In the standard search for the pair production of charginos, the final state can become effectively invisible when the mass difference between the sneutrino and the chargino is less than about $3\,\mathrm{GeV}/c^2$ [10, 11]. It was pointed out in [12] that this "blind spot" might partially be covered by the search for the mixed Supersymmetric/Standard Model final state of W pair production, where one W boson decays to chargino and neutralino, the chargino decaying to a sneutrino and a lepton (with an energy too small to be detected), while the other W boson decays to Standard Model particles. This topology will hereafter be called single visible W bosons. The search for single visible W bosons in W pair production leads naturally to a determination of the invisible branching ratio (or partial width) of the W boson.

This paper is organized as follows. After a description of the ALEPH detector and the Monte Carlo samples, the measurement of the single W production cross section is discussed in section 4. The search for single visible W bosons is described in section 5, followed by the conclusions. The results presented in this paper are obtained using data recorded with the ALEPH detector at centre-of-mass energies of 161.3, 172.1 and 182.7 GeV, referred to hereafter as 161, 172 and 183 GeV, with integrated luminosities of 11.1, 10.8 and $57\,\mathrm{pb}^{-1}$, respectively.

2 The ALEPH Detector

The ALEPH detector is described in detail in Ref. [13], and its performance as well as the standard analysis algorithms are given in Ref. [14]. Here only the parts relevant to this analysis are described briefly.

The tracking system consists of a silicon vertex detector (VDET), a cylindrical drift chamber (ITC) and a large time projection chamber (TPC), all situated in a 1.5 Tesla magnetic field provided by a superconducting solenoidal coil. The tracking system achieves a transverse momentum resolution of $\Delta P_T/P_T = 6 \times 10^{-4} P_T$ (P_T in GeV/c).

A highly granular electromagnetic calorimeter (ECAL) situated between the TPC and the coil is used to identify electrons and photons and measure their energies. The ECAL achieves an energy resolution of $\sigma_E/E = 0.18/\sqrt{E(GeV)}$ for isolated electrons and photons. At low polar angles, luminosity calorimeters (SiCAL and LCAL) extend the coverage of the ALEPH detector down to 34 mrad. The hadron calorimeter (HCAL) consists of the iron return yoke of the magnet instrumented with streamer tubes. It provides a measurement of hadronic energy with the energy resolution of $\sigma_E/E = 0.85/\sqrt{E(GeV)}$. The HCAL is complemented by outer muon chambers.

The tracking and calorimetry information is combined in an energy flow algorithm providing a list of objects classified as tracks, photons and neutral hadrons [14]. Particle tracks, with a polar angle greater than 18.2°, which originate from within a cylinder of 2 cm radius and 20 cm length, centered on the nominal interaction point are defined as *good tracks*. Leptons are identified as electrons by their shower's longitudinal and transverse energy distribution in the ECAL. Muons are identified by their penetration power via their hit pattern in the HCAL and associated hits in the muon chambers.

3 Monte Carlo Samples

Fully simulated Monte Carlo event samples reconstructed with the same program as the data were used for the design of the selections, determination of signal efficiency and the estimation of the background. Signal samples and all major background sources correspond to at least 20 times the collected luminosity.

The GRC4F program [15] was used as a Monte Carlo generator for the single W signal. The effective QED coupling constant $\alpha_{QED} = 1/130.2$ was used, following the suggestion in Ref. [16]. For initial state radiation, the photon structure function approach was utilized. Final state radiation was simulated with the PHOTOS [17] package. Tau decays were handled by TAUOLA [18]. Signal events were also generated with PYTHIA for cross checks [19].

Two-fermion events were generated with PYTHIA ($q\bar{q}$), UNIBAB (e^+e^-) [20] and KORALZ [21] ($\mu^+\mu^-$, $\tau^+\tau^-$). W pair production events were generated with KORALW [22]. PYTHIA was used to generate four-fermion events (Zee, ZZ). PHOT02 [23] and PYTHIA were used to simulate two-photon processes.

To simulate the mixed Standard Model/Supersymmetric decay in W pair production, W pair events were generated with KORALW. One of the W boson decays was replaced by an isotropic decay to chargino and neutralino, followed by the chargino decay to a lepton and a sneutrino.

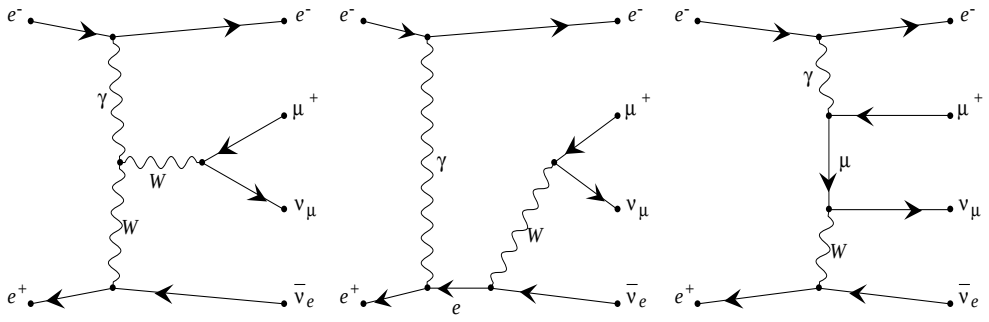

Figure 1: Dominant t-channel diagrams for the process of $e^+e^- \to e^-\bar{\nu}_e\mu^+\nu_\mu$.

4 Single W Boson Production Cross Section

The dominant diagrams of the four-fermion process of single W production are shown in Fig. 1 for the $e\nu\mu\nu$ final state. The first diagram is sensitive to the WWγ coupling; the equivalent diagram with the WWZ coupling is strongly suppressed due to the large mass of the Z boson. The outgoing electron is predominantly emitted at small polar angles. To suppress the contribution from other four-fermion processes, which give rise to the same final states, but whose characteristics are different from the single W process, the single W signal is defined at the generator level as

$$\begin{cases} \vartheta_{\mathrm{e}} & < & 34\,\mathrm{mrad}, & \\ \mathrm{E}_\ell & > & 20\,\mathrm{GeV} \;\text{ and }\; |\cos\vartheta_\ell| < 0.95 & \text{for the leptonic decay,} \\ \mathrm{M}_{\mathrm{q\bar{q}'}} & > & 60\,\mathrm{GeV}/c^2 & \text{for the hadronic decay,} \end{cases}$$

where ϑ_{e} is the polar angle of the scattered electron and E_ℓ and ϑ_ℓ are the energy and polar angle of the charged lepton from the W decay; $\mathrm{M}_{\mathrm{q\bar{q}'}}$ is the invariant mass of the quark pair.

As $\vartheta_{\mathrm{e}} = 34\,\mathrm{mrad}$ corresponds to the lower edge of the angular acceptance of the ALEPH detector, the outgoing electron escapes undetected (untagged). Two distinct topologies are identified: for the leptonic decays of the W boson a single lepton will be observed, whereas for the hadronic decays an acolinear and acoplanar hadronic system with the mass of the W boson is expected.

4.1 Leptonic Selection

In leptonic decays of the W boson, a single track is expected from the electron, muon or single-prong tau decay. A higher multiplicity is expected for other tau decays. Therefore, events with one or three good tracks are accepted and the visible mass must be less than $5\,\mathrm{GeV}/c^2$.

The polar angle of the missing momentum direction is required to be greater than 25.8°. To reject tagged two-photon events, the energy E_{12} measured within a cone of 12° around the beam axis is required to be zero.

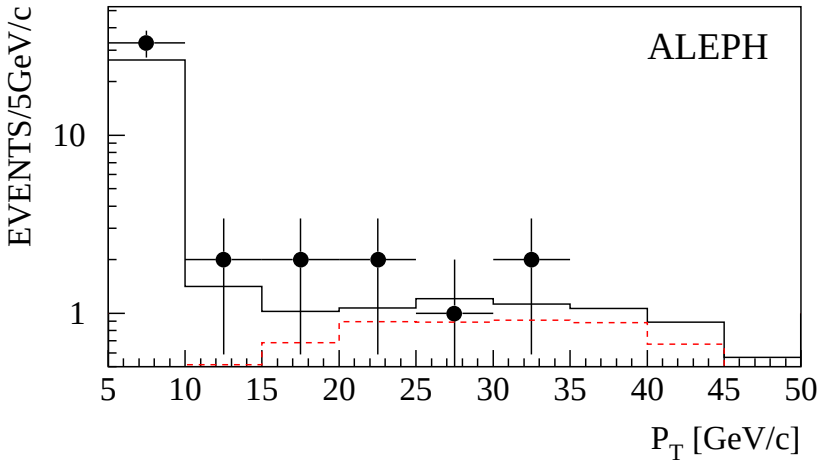

Figure 2: The transverse momentum distribution for data (points) and Monte Carlo (solid histogram) at 183 GeV. The signal Monte Carlo is shown as a dashed histogram. Several cuts were loosened to ensure sufficient statistics for this plot.

The remaining backgrounds, mainly untagged two-photon events and two-fermion events, are eliminated with the requirement that the transverse missing momentum be greater than $6\%\sqrt{s}$. This threshold is increased to $10\%\sqrt{s}$ if the missing momentum direction points within 10° in azimuth to the boundaries between the two LCAL halves or the six inner sectors of the TPC. The data agree well with the Standard Model Monte Carlo as shown in Fig. 2 for the transverse missing momentum distribution. It is required that no energy be found within a wedge of 10° opposite to the direction of the transverse momentum reconstructed from charged tracks (large angle neutral energy veto). The selection criteria described up to this point constitute the core of the leptonic analysis, which hereafter will be referred to as the leptonic kernel.

At this point the remaining background is Zee with the Z boson decaying to neutrinos. It is reduced by taking advantage of the softer lepton spectrum with respect to the signal. Events containing an identified electron with an energy less than 20 GeV are rejected, where the energy is defined as the sum of track energy and neutral objects in a cone of 10°.

The selection efficiencies for the three leptonic W boson decay modes are 81% for electron, 82% for muon and 48% for tau. The expected background amounts to 38 fb at 161 GeV, 41 fb at 172 GeV and 55 fb at 183 GeV, dominated by the process Zee. In the data, 11 events are observed, in agreement with the expectation from the Standard Model of 10.9 events (3.8 events background). Five events with an electron or muon are selected, where 8.4 events are expected.

The inefficiency due to unsimulated beam-related background, measured with events recorded at random beam crossings, amounts to 4% at 161 GeV, 2% at 172 GeV and 4.6% at 183 GeV.

4.2 Hadronic Selection

To select the hadronic decay of the W boson, at least seven good tracks are required. The polar angle of the missing momentum must be greater than 25.8° to suppress the background from $q\bar{q}$ events. Tagged two-photon events and two-fermion events with initial state radiation are rejected by demanding that the energy E_{12} be less than $2.5\%\sqrt{s}$. Untagged two-photon events are rejected by requiring that the visible mass exceed $60\,\mathrm{GeV}/c^2$. The visible mass is required to be less than $90\,\mathrm{GeV}/c^2$ to reject ZZ events.

Events are rejected if the energy in a wedge of 30° centred on the transverse missing momentum direction is greater than $10\%\sqrt{s}$. The acollinearity angle between the two hemisphere momentum directions is required to be less than 165°.

The semileptonic final state ($\ell\nu q\bar{q}'$) of W pair production is efficiently rejected by requiring that no identified electron or muon with an energy of more than $5\%\sqrt{s}$ be reconstructed. The selection criteria described up to this point will be referred to hereafter as the hadronic kernel.

To reject semileptonic decays of W pairs in which the charged lepton is a tau, the tau jet is reconstructed as described in [24]. The event is rejected if a tau jet is reconstructed with a charged energy of more than $2.5\%\sqrt{s}$ and if the invariant mass of the hadronic system, excluding the tau jet, is greater than $60\,\mathrm{GeV}/c^2$ or if the angle between the two quark jets is greater than 150° at 161 GeV, 130° at 172 GeV or 100° at 183 GeV. The latter cut decreases with the centre-of-mass energy because the boost of the W boson increases.

The efficiency for the hadronic W channel is typically about 40%. The background amounts to 69 fb at 161 GeV, 164 fb at 172 GeV and 188 fb at 183 GeV, dominated by W pair production. The largest contribution to the systematic error is the statistical precision of the background determination (10%).

In this channel, 21 events are selected in the data, in agreement with 21.2 events (13.1 events background) predicted by the Standard Model.

4.3 Results

Due to the limited statistics accumulated so far, the energy dependence and the flavour composition of the final states arising from single W production are assumed according to the Standard Model in deriving the results. The single W cross section at 183 GeV is determined to be

$$\sigma_{\mathrm{W}} = 0.41 \pm\ 0.17(\mathrm{stat.}) \pm\ 0.04(\mathrm{syst.})\ \mathrm{pb}.$$

The measurement agrees well with the Standard Model expectation of 0.41 pb calculated with GRC4F. The dominant contribution to the systematic error is the uncertainty on the background estimation for the hadronic channel.

The generators PYTHIA and GRC4F were compared for the signal simulation. They differ significantly in the prediction of the cross section, traced back to the P_T spectrum of the outgoing electron. However, the resulting efficiencies agree reasonably well. The measurement of the cross section therefore does not depend strongly on the generator used.

While single W production is sensitive to the WWγ coupling, W pair production, the dominant background, depends both on the WWγ and the WWZ vertex. A conservative

approach in setting limits is to fix the background expectation to its Standard Model value. Any variation therefore is entirely attributed to the WWγ vertex in single W production.

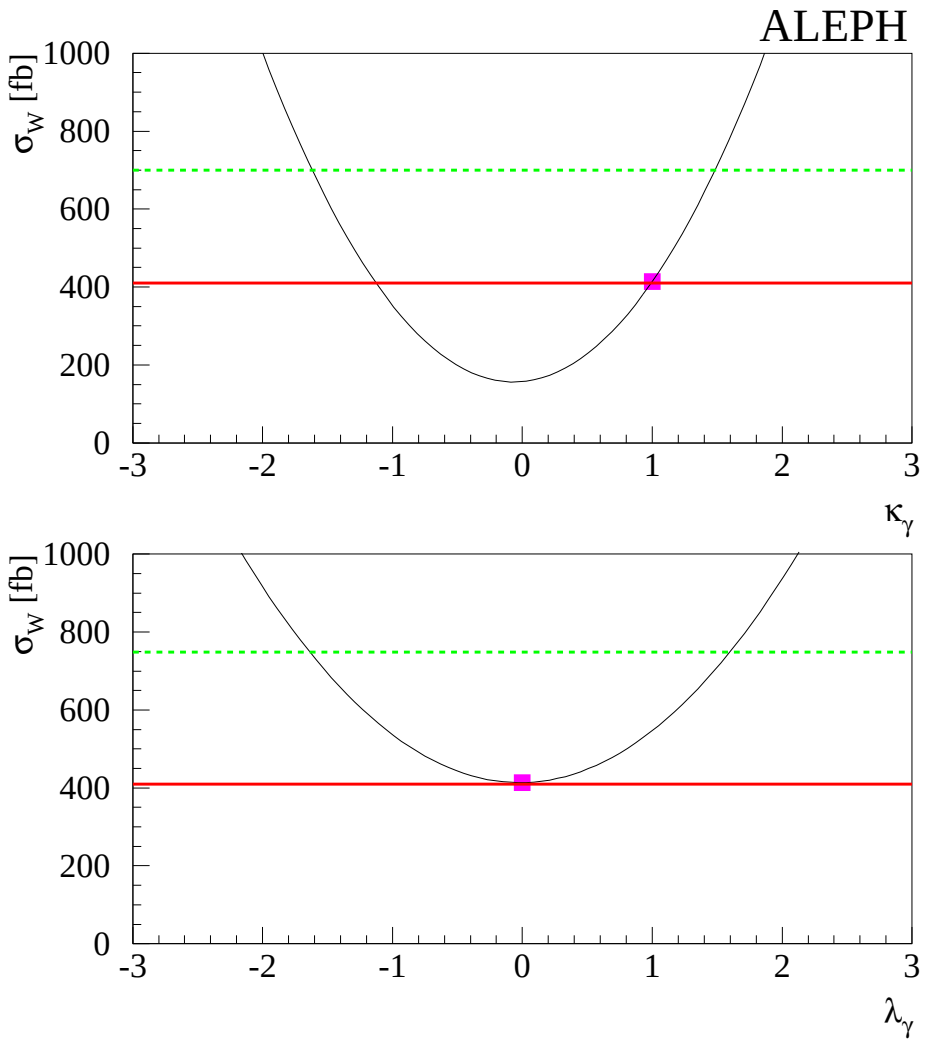

Figure 3: The single W total cross section calculated with GRC4F as function of (top) $\kappa_\gamma(\lambda_\gamma = 0)$ and (bottom) $\lambda_\gamma(\kappa_\gamma = 1)$. The horizontal solid line indicates the measured cross section, the dashed line the upper limit on the cross section at 95% C.L. The Standard Model expectation is denoted by the square.

The measured cross section is translated into an upper limit on the production cross section taking into account the physically allowed cross section region, following the prescription of [25]. This procedure is performed while varying one coupling at a time. The 95% C.L. limits on κ_γ and λ_γ, shown in Fig. 3 are

$$\begin{aligned} -1.6 \;<\; \kappa_\gamma \;<\; 1.5 \quad (\lambda_\gamma \;=\; 0), \\ -1.6 \;<\; \lambda_\gamma \;<\; 1.6 \quad (\kappa_\gamma \;=\; 1). \end{aligned}$$

The L3 collaboration has reported on a study of single W production at LEP2 for energies between 130 and 183 GeV [26]. The DELPHI [5] collaboration has analysed WW and

eνW production jointly. ALEPH has measured the couplings at the WWγ vertex with single γ production ($e^+e^- \to \nu\bar{\nu}\gamma$) for energies up to 183 GeV [27]. At hadron colliders, by measuring Wγ production, UA2 [28], CDF [29] and D0 [30] have a higher sensitivity for λ_γ compared to LEP.

5 Search for Single Visible W Bosons

In W pair production, effectively invisible decays of the W boson can be tagged by the decay of the other W boson to Standard Model particles. An example is the decay of the W boson to supersymmetric particles: a W boson decays to chargino and neutralino, followed by the chargino decay to sneutrino and lepton. The supersymmetric decay of the W boson becomes effectively invisible if the chargino and sneutrino are mass degenerate.

The final state topologies for the mixed Standard Model/Supersymmetric decay mode of W pair production are defined by the mass difference ΔM between the chargino and sneutrino: $\Delta M \approx 0$ is hereafter referred to as the degenerate case and $\Delta M = 3\,\mathrm{GeV}/c^2$ as the nondegenerate case.

Three distinct selections are necessary: single leptons (degenerate case), acoplanar leptons (nondegenerate case), and a hadronic selection (for both cases). With the exception of the acoplanar lepton case, the topologies closely resemble the single W process discussed in the previous section. The main issue for the selections is therefore the rejection of the single W background.

5.1 Single Lepton Selection

In the single lepton analysis the leptonic kernel is used. The lepton is required to be identified as an electron or a muon.

In the signal the lepton originates from a two-body W decay, while in the single W background the W boson recoils against an eν system leading to a broader distribution of the lepton energy. The energy of the lepton is therefore required to be greater than 32 GeV and less than 52 GeV at 161 GeV; the window is enlarged at 172 GeV from 26 GeV to 60 GeV and finally, at 183 GeV, the energy must be greater than 24 GeV and less than 70 GeV.

Typically, an efficiency of about 71% is obtained. The background is dominated by the single W and Zee processes. The background is lowest at 161 GeV (36 fb) and increases to 66 fb and 96 fb at 172 GeV and 183 GeV.

In the data, 2 events are selected, where 7.3 are expected from background processes. This result reflects the deficit of electrons and muons observed in the single W cross section measurement. One event is a single muon event at 172 GeV. The other event is observed at 183 GeV and has a single electron.

5.2 Acoplanar Lepton Selection

In the acoplanar lepton analysis, two or four good tracks are required and the smallest triplet mass, interpreted as a tau decay, must be less than $1.5\,\mathrm{GeV}/c^2$. The acoplanarity angle of the two leptons must be less than 170° to reject two-fermion events. To reject

background events with initial state radiation while retaining signal events with final state radiation, a photon veto is applied. If a neutral object is reconstructed with an energy of more than 4 GeV, separated from each of the two leptons by more than 10° and if its invariant mass with each of the leptons is greater than 2 GeV/c^2, then the event is rejected. The acollinearity angle of the two leptons is required to be greater than 10°.

To reject the tagged two-photon background, the energy E_{12} is required to be zero. Untagged two-photon events are vetoed by requiring the transverse missing momentum to be greater than $10\%\sqrt{s}$.

As in the single lepton analysis, the leading lepton is required to be identified as an electron or a muon. Its energy must fall in the same ranges as for the single lepton case.

At this point the dominant background is (Standard Model) W pair production. In the signal the least energetic lepton is expected to be soft and so the energy of the lepton, i.e., the track energy plus the neutral objects in a cone of 10° around it, is required to be less than 5 GeV.

For $\Delta M = 3\,\mathrm{GeV}/c^2$ and a chargino mass of $45\,\mathrm{GeV}/c^2$, the efficiency at the lowest centre-of-mass energy is 65%, decreasing to 59% and 54% at 172 GeV and 183 GeV due to the increased boost of the chargino. As the background is dominated by W pair production, the background increases from 12 fb at 161 GeV to 38 fb and 44 fb at 172 GeV and 183 GeV.

For the sum of the three centre-of-mass energies, a total background of 2.9 events is expected. In the data, no events are selected.

5.3 Hadronic Selection

The hadronic selection starts with the hadronic kernel of the single W analysis. To cope with the variation of the mass difference ΔM in an optimal way, the tau jet veto is applied with a *sliding* threshold of $(2.5 + 0.2\Delta M)\%\sqrt{s}$ on the charged energy of the tau jet. The same cuts as in section 4.2 are then applied on the invariant mass of the hadronic jets and their acollinearity angle.

The missing mass is required to be greater than $70\,\mathrm{GeV}/c^2$ and less than $100\,\mathrm{GeV}/c^2$ as the recoil mass of the signal is expected to be about the mass of the W boson. The missing mass distribution for the signal, the Standard Model Monte Carlo and the data is shown in Fig. 4.

The efficiency for the degenerate (nondegenerate) case is estimated to be 30% (24%) at 161 GeV, 39% (37%) at 172 GeV and 41% (33%) at 183 GeV. Far above the W pair production threshold, the background increases substantially from 70 fb (73 fb) at 161 GeV to 188 fb (206 fb) and 209 fb (235 fb) at 172 GeV and 183 GeV for the degenerate (nondegenerate) case.

In the data, 1 event is selected at 161 GeV, 3 events at 172 GeV and 10 events at 183 GeV, where 0.8, 2.2 and 13.4 events, respectively, are expected for the loosest cuts, i.e., $\Delta M = 3\,\mathrm{GeV}/c^2$. The tightest cuts, corresponding to the mass degenerate case, accept the same events in the data, while the background expectation is reduced to 0.8, 2.0 and 11.9 events, respectively.

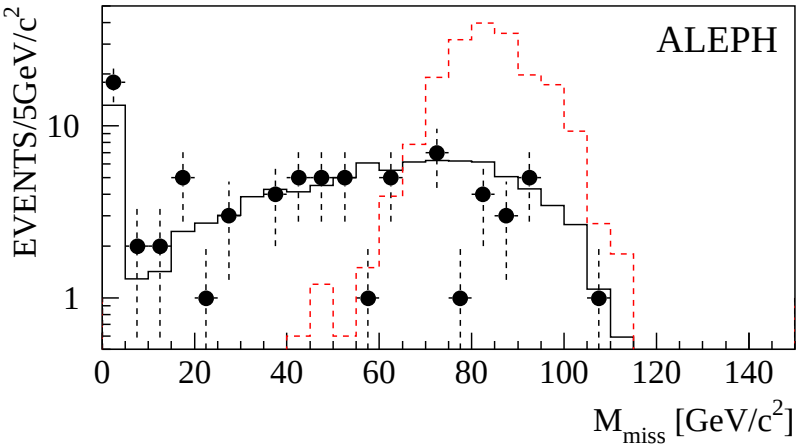

Figure 4: The missing mass distribution for data (points) and Monte Carlo (solid histogram) at 183 GeV. The signal Monte Carlo in arbitrary normalisation is shown as dashed histogram. Several cuts were loosened to ensure sufficient statistics for this plot.

5.4 Results

No excess of candidate events with respect to the Standard Model expectation is observed. Therefore limits on the branching ratio of the W boson are calculated.

Conservatively, only irreducible physics backgrounds are subtracted: the single W process in the single lepton selection and single W and W pair production in the hadronic selection. The background estimation is reduced by the statistical error of the Monte Carlo sample. The signal efficiencies are reduced by 3% to take into account the systematic error, which is dominated by the limited Monte Carlo statistics and lepton identification efficiency. This procedure leads to a subtractable background of at most 14.3 events ($\mathcal{B}_{\rm susy} = 0$), where 16 events are selected in data.

The cross sections used in the calculation of the limit are reduced by 2% in order to take into account the variation of the total WW cross section as a function of the total width (including the new channel) and the general theoretical uncertainty. Limits at 95% C.L. on the W boson supersymmetric branching ratio are then obtained as ($\mathcal{B}_{\rm susy} + \mathcal{B}_{\rm SM} = 1$)

$$\begin{aligned} \mathcal{B}_{\rm susy}(\Delta{\rm M} \approx 0) &< 1.3\,\%, \\ \mathcal{B}_{\rm susy}(\Delta{\rm M} = 3\,{\rm GeV}/c^2) &< 1.9\,\%, \end{aligned}$$

assuming $\mathcal{B}(\chi^\pm \to \ell\tilde{\nu}) = 100\%$ and $m_{\chi^\pm} = 45\,{\rm GeV}/c^2$, $m_\chi = 22\,{\rm GeV}/c^2$.

The minimal supersymmetric extension of the Standard Model is governed by a few parameters, among them μ, a supersymmetric Higgs mass term, and the ratio of the vacuum expectation values of the two Higgs doublets $\tan\beta$. The supersymmetry breaking mass terms $\rm M_2$ and $\rm M_1$ are related via the unification condition $\rm M_1 = 5/3 \tan^2\vartheta_W M_2$ for the following.

A typical example for the "blind spot" is $\mu = -200\,{\rm GeV}/c^2$ and $\tan\beta = 2$. The limit on the branching ratio as a function of the gaugino mass parameter $\rm M_2$ is shown in Fig. 5; $m_{\chi^\pm} < 51\,{\rm GeV}/c^2$ is excluded at 95% C.L. under the assumptions mentioned above. The reduction of the cross section due to the production of massive particles is taken into account in this limit.

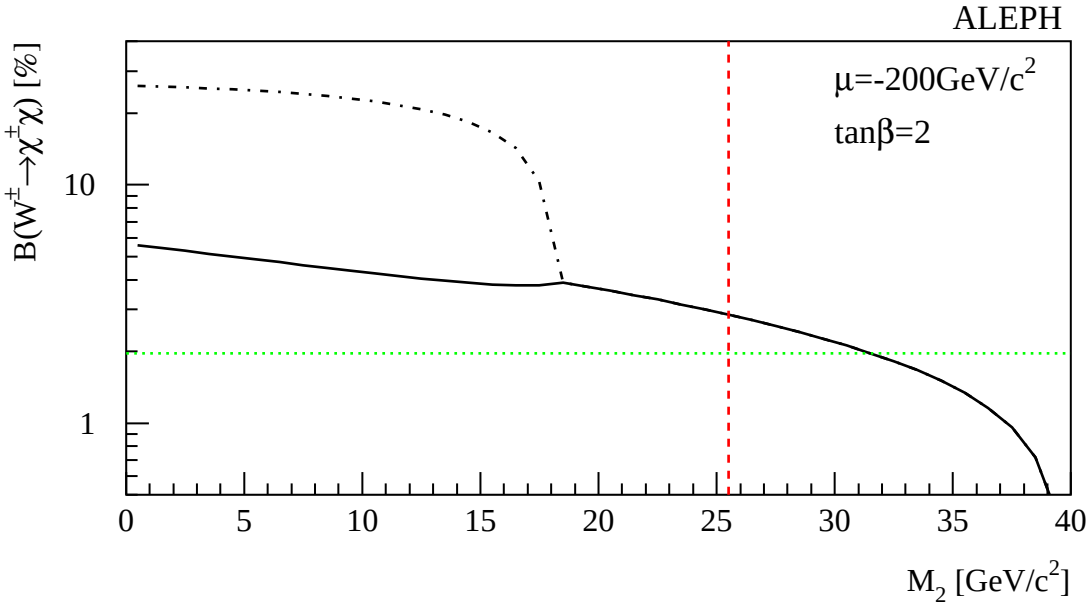

Figure 5: Branching ratio of W to $\chi^{\pm}\chi$ (solid curve) for $\mu = -200\,\mathrm{GeV}/c^2$, $\tan\beta = 2$ and $\Delta\mathrm{M} < 3\,\mathrm{GeV}/c^2$. The branching ratio limit is the dotted line. The dashed line is the LEP1 chargino mass limit. The sum of the branching ratios $\mathcal{B}(\mathrm{W} \to \chi^{\pm}\chi)+\mathcal{B}(\mathrm{W} \to \chi^{\pm}\chi')$ (dash-dotted curve) is also shown.

Even though the search for effectively invisible W bosons is driven by the supersymmetric scenario, it must be noted that the limit on the branching ratio in the degenerate case is fairly model independent. As long as a model yields no reconstructable track, the knowledge of the underlying model to create a effectively invisible decay of the W boson is not necessary.

The definition of the degenerate case is identical to that used in Ref. [31], where a limit of 139 MeV was determined indirectly by the measurement of the W pair production cross section. The combination of the measurements of the four LEP experiments improves the result to 41 MeV [32]. A limit on the invisible W decay width of 109 MeV was obtained from measurements of the weak boson production rates at the Tevatron combined with the Z data at LEP and the Standard Model prediction for the leptonic branching ratio [32]. These limits can be compared directly to the limit obtained in this paper, translated into a limit on the partial width: 27 MeV.

6 Conclusions

Single W production has been studied in the data recorded with the ALEPH detector at centre-of-mass energies up to 183 GeV. The single W production cross section is measured to be $\sigma_{\mathrm{W}} = 0.41 \pm 0.17(\mathrm{stat.}) \pm 0.04(\mathrm{syst.})$ pb, in agreement with the Standard Model expectation. From this measurement, limits at 95% C.L. on the WWγ couplings, $-1.6 < \kappa_\gamma < 1.5$ ($\lambda_\gamma = 0$) and $-1.6 < \lambda_\gamma < 1.6$ ($\kappa_\gamma = 1$), are deduced.

A search for single visible W bosons was performed, leading to a limit on the invisible

branching ratio of the W boson of 1.3% (or equivalently $\Gamma_{\rm inv} = 27\,{\rm MeV}$) at 95% C.L. For a particularly difficult point ("blind spot") in the parameter space of the MSSM ($\tan\beta = 2$, $\mu = -200\,{\rm GeV}/c^2$ and $0 < m_{\chi^\pm} - m_{\tilde{\nu}} < 3\,{\rm GeV}/c^2$), charginos with masses up to $51\,{\rm GeV}/c^2$ are excluded.

Acknowledgements

We would like to thank Y. Kurihara and T. Sjöstrand for helpful discussions on GRC4F and PYTHIA. J. Kalinowski and P.M. Zerwas are kindly acknowledged for discussions on the supersymmetric decay of W bosons. We wish to congratulate the accelerator divisions at CERN for the very successful operation of LEP. We are also grateful to the engineers and technicians in our institutions for their contribution to the successful operation of the ALEPH detector. Those of us from non-member countries thank CERN for its hospitality.

References

[1] The LEP Collaborations, *A combination of Preliminary Electroweak Measurements and Constraints on the Standard Model*, CERN-EP/99-015.

[2] *Physics at LEP2*, CERN 96-01, edited by G. Altarelli, T. Sjöstrand and F. Zwirner, vol. 1, 525.

[3] H. Aronson, Phys. Rev. **186** (1969) 1434; K.J. Kim and Y.-S. Tsai, Phys. Rev. **D7** (1973) 3710.

[4] ALEPH Collaboration, *Measurement of Triple Gauge Boson Couplings at 172 GeV*, Phys. Lett. **B422** (1998) 369.

[5] DELPHI Collaboration, *Measurement of Trilinear Gauge Couplings in e^+e^- Collisions at 161 GeV and 172 GeV*, Phys. Lett. **B423** (1998) 194.

[6] L3 Collaboration, *Measurements of Mass, Width and Gauge Couplings of the W Boson at LEP*, Phys. Lett. **B413** (1997) 176.

[7] OPAL Collaboration, *W^+W^- Production and Triple Gauge Boson Couplings at LEP Energies up to 183 GeV*, Euro. Phys. J. **C8** (1999) 191.

[8] T. Tsukamoto and Y. Kurihara, Phys. Lett. **B389** (1996) 162.

[9] For a compilation of review articles see *Supersymmetry and Supergravity*, Ed. M. Jacob, North-Holland and World Scientific, 1986.

[10] ALEPH Collaboration, *Mass Limit for the Lightest Neutralino*, Z. Phys. **C72** (1996) 549.

[11] ALEPH Collaboration, *Searches for Charginos and Neutralinos in e^+e^- Collisions at $\sqrt{s} = 161$ and 172 GeV*, Euro. Phys. J. **C2** (1998) 417.

[12] J. Kalinowski and P.M. Zerwas, Phys. Lett. **B400** (1997) 112.

[13] ALEPH Collaboration, *ALEPH: A Detector for Electron - Positron Annihilations at LEP*, Nucl. Instrum. Meth. **A294** (1990) 121.

[14] ALEPH Collaboration, *Performance of the ALEPH Detector at LEP*, Nucl. Instrum. Meth. **A360** (1995) 481.

[15] J. Fujimoto *et al.*, Comp. Phys. Comm. **100** (1997) 128.

[16] K. Hagiwara *et al.*, Nucl. Phys. **B365** (1991) 544.

[17] E. Barberio *et al.*, Comp. Phys. Comm. **66** (1991) 115, **79** (1994) 291.

[18] S. Jadach *et al.*, Comp. Phys. Comm. **70** (1992) 69, **76** (1993) 361.

[19] T. Sjöstrand, Comp. Phys. Comm. **82** (1994) 74; CERN-TH 7112/93 (1993, revised August 1994).

[20] H. Anlauf *et al.*, Comp. Phys. Comm. **79** (1994) 466.

[21] S. Jadach, B.F.L. Ward and Z. Wąs, Comp. Phys. Comm. **79** (1994) 503.

[22] M. Skrzypek, S. Jadach, W. Placzek and Z. Wąs, Comp. Phys. Comm. **94** (1996) 216.

[23] J.A.M. Vermaseren, in *Proceedings of the IVth International Workshop on Gamma Gamma Interactions*, edited by G. Cochard and P. Kessler, Springer Verlag (1980) 35; ALEPH Collaboration, *An Experimental Study of $\gamma\gamma \to$ Hadrons at LEP*, Phys. Lett. **B313** (1993) 509.

[24] ALEPH Collaboration, *Measurement of the W Mass in e^+e^- Collisions at Production Threshold*, Phys. Lett. **B401** (1997) 347.

[25] Particle Data Group, Phys. Rev. **D54** (1996) 159.

[26] L3 Collaboration, *Production of Single W Bosons in e^+e^- Interactions at 130 GeV$\leq \sqrt{s} \leq$183 GeV and Limits on anomalous $WW\gamma$ Couplings*, Phys. Lett. **B436** (1998) 417.

[27] ALEPH Collaboration, *Measurement of Triple Gauge $WW\gamma$ Couplings at LEP2 using Photonic Events*, Phys. Lett. **B445** (1998) 239.

[28] UA2 Collaboration, *Direct Measurement of the $W\gamma$ Coupling at the CERN $\bar{p}p$ Collider*, Phys. Lett. **B277** (1992) 194.

[29] CDF Collaboration, *Measurement of W-Photon Couplings in $p - \bar{p}$ Collisions at $\sqrt{s} = 1.8$ TeV*, Phys. Rev. Lett. **74** (1995) 1936.

[30] D0 Collaboration, *Limits on Anomalous $WW\gamma$ and WWZ Couplings*, Phys. Rev. **D58** (1998) 31102.

[31] ALEPH Collaboration, *Measurement of W-pair Production in e^+e^- Collisions at 183 GeV*, Phys. Lett. **B453** (1999) 107.

[32] D. Karlen, *Experimental Status of the Standard Model*, plenary talk given at the XXIX International Conference on High Energy Physics, July 23-29, 1998, Vancouver, Canada.